Supplementary Material for "Identifying Integer-Variable-Induced Disjointness Within Security Region Considering Unit Commitment Adjustments"

Zhirou Wang, *Student Member*, *IEEE*, Zhengshuo Li, *Senior Member*, *IEEE*, Tao Niu, *Senior Member*, *IEEE*, and Lin Xue, *Member*, *IEEE*

APPENDIX

A. Proof of Convergence of LEC-Based Iterative Refinement

Let the continuous relaxation of the SR under UC adjustments be denoted as $\mathcal{E}_{\mathrm{SR}}^{\mathcal{Z}}$, and let $\mathcal{Z}$ denote the finite set of all possible quick-start unit combinations (UC configurations). Define the iterative infeasible subregion sequence as

$$\mathcal{I}_{\mathrm{IR}}^{(0)} = \mathcal{E}_{\mathrm{SR}}^{\mathcal{Z}} \bigcap \mathrm{LEC}(\boldsymbol{Z}^*), \tag{A1}$$

$$\mathcal{I}_{\mathrm{IR}}^{(i+1)} = \mathcal{I}_{\mathrm{IR}}^{(i)} \bigcap \mathrm{LEC}^{(i+1)}, \tag{A2}$$

where $\mathrm{LEC}^{(i+1)} = \{\boldsymbol{X}: \boldsymbol{\lambda}_{(i+1)}^{\mathrm{T}} \boldsymbol{A}\boldsymbol{X} \le \boldsymbol{\lambda}_{(i+1)}^{\mathrm{T}} (\boldsymbol{D} - \boldsymbol{C}\boldsymbol{Z}_{(i+1)}^*)\}$ is the LEC constructed from the infeasible pair $(\boldsymbol{X}^*, \boldsymbol{Z}_{(i+1)}^*)$ according to **Lemma 1**. To prove the convergence of LEC-based iterative refinement, the following properties are demonstrated.

Property 1 (*Inclusiveness*): **Each** LEC **contains the detected infeasible point** $\boldsymbol{X}^*$.

Proof: Since the infeasible point $\boldsymbol{X}^*$ has been identified by the **RDD**, there exists no $(\boldsymbol{Y}, \boldsymbol{Z}) \in \mathcal{Y} \times \mathcal{Z}$ such that $\boldsymbol{A}\boldsymbol{X}^* + \boldsymbol{B}\boldsymbol{Y} + \boldsymbol{C}\boldsymbol{Z} \le \boldsymbol{D}$. Fix a UC configuration $\boldsymbol{Z}_{(i+1)}$. The infeasibility of the linear system $\boldsymbol{B}\boldsymbol{Y} \le \boldsymbol{D} - \boldsymbol{A}\boldsymbol{X}^* - \boldsymbol{C}\boldsymbol{Z}_{(i+1)}$ implies, by Farkas-Lemma, that there exists a nonnegative multiplier $\boldsymbol{\lambda} \ge \boldsymbol{0}$ such that $\boldsymbol{\lambda}^{\mathrm{T}}\boldsymbol{A}\boldsymbol{X}^* > \boldsymbol{\lambda}^{\mathrm{T}}(\boldsymbol{D} - \boldsymbol{C}\boldsymbol{Z}_{(i+1)})$. Accordingly, the associated LEC is defined as

$$\mathrm{LEC}^{(i+1)} = \{\boldsymbol{X}: \boldsymbol{\lambda}^{\mathrm{T}}\boldsymbol{A}\boldsymbol{X} \ge \boldsymbol{\lambda}^{\mathrm{T}}(\boldsymbol{D} - \boldsymbol{C}\boldsymbol{Z}_{(i+1)})\}. \tag{A3}$$

Since the strict inequality implies the non-strict form, it follows that $\boldsymbol{X}^* \in \mathrm{LEC}^{(i+1)}$. Therefore, each cut LEC is guaranteed to contain the already-detected infeasible point $\boldsymbol{X}^*$. It is emphasized that the infeasibility of $\boldsymbol{X}^*$ is established prior to and independently of the LEC construction. The role of the LEC is to geometrically enclose the infeasible point $\boldsymbol{X}^*$ and extend its exclusion to a local half-space. ∎

Property 2 (*Monotonicity*): **Sequence** $\{\mathcal{I}_{\mathrm{IR}}^{(i)}\}$ **is monotonically non-expanding and converges in a finite number of iterations**.

Proof: Since each iteration introduces one additional LEC, it follows directly that

$$\mathcal{I}_{\mathrm{IR}}^{(i+1)} = \left(\mathcal{I}_{\mathrm{IR}}^{(i)} \bigcap \mathrm{LEC}^{(i+1)}\right) \subseteq \mathcal{I}_{\mathrm{IR}}^{(i)}. \tag{A4}$$

Let z denote the total number of UC configurations in $\mathcal{Z}$, corresponding to all possible on/off combinations of quick-start units. At each iteration, the *detect-and-refine* step identifies at least one new configuration $\boldsymbol{Z}_{(i+1)}^* \in \mathcal{Z}$, introducing a unique exclusion cut $\mathrm{LEC}^{(i+1)}$. Since $\mathcal{Z}$ is finite and each iteration identifies one distinct component associated with a specific UC configuration $\boldsymbol{Z}_{(i+1)}^*$, the iterative process must terminate after at most z iterations, i.e.,

$$\lim_{i \to i^*} \mathcal{I}_{\mathrm{IR}}^{(i)} \subseteq \mathcal{I}_{\mathrm{IR}}^{(*)}, i^* \le z. \tag{A5}$$

Hence, the LEC-based iterative refinement converges finitely to the complete local infeasible subregion $\mathcal{I}_{\mathrm{IR}}^{(*)}$. ∎

Property 3 (*Accuracy*): **no feasible points are erroneously included in** $\mathcal{I}_{\mathrm{IR}}^{(*)}$.

Proof: Recall Step a) **Infeasibility effectiveness detection**. In each iteration, the IISI procedure examines whether there exists a candidate point $\boldsymbol{X} \in \mathcal{I}_{\mathrm{IR}}^{(i)}$ and a UC configuration $\boldsymbol{Z}$ such that the minimum-slack problem in (10) attains a zero optimal value. A new $\mathrm{LEC}^{(i+1)}$ is constructed only when a feasible pair $(\boldsymbol{X}_{(i)}^*, \boldsymbol{Z}_{(i)}^*)$ is detected from (6). When $\mathcal{I}_{\mathrm{IR}}^{(*)}$ converges, for any $\boldsymbol{X} \in \mathcal{I}_{\mathrm{IR}}^{(*)}$ and all UC configurations $\boldsymbol{Z}$, the minimum-slack problem (10) yields a strictly positive optimal value, certifying that no feasible redispatch $\boldsymbol{Y}$ exists for any such $(\boldsymbol{X}, \boldsymbol{Z})$. Consequently, no additional LEC can be generated, and $\mathcal{I}_{\mathrm{IR}}^{(*)}$ contains no feasible points. Therefore, the accuracy property is guaranteed by the algorithmic verification mechanism of the IISI procedure. ∎

Therefore, the LEC-based iterative refinement process is both monotonically non-expanding and finitely convergent, producing the complete infeasible subregion that satisfies **Properties 1-3**.

B. Pseudocode of the IISI Algorithm

IISI Algorithm: Identifying Disjoint Regions Within $\Omega_{\mathrm{SR}}^{\mathcal{Z}}$

1. *initialization*: Input parameter $\boldsymbol{A}$, $\boldsymbol{B}$, $\boldsymbol{C}$ and $\boldsymbol{D}$, outer convex relaxation $\mathcal{E}_{\mathrm{SR}}^{\mathcal{Z}}$, set $\mathcal{I}_{\mathrm{IR}} = \emptyset$, and accuracy threshold $\epsilon > 0$;
2. **if** $\Pi^+(\mathcal{E}_{\mathrm{SR}}^{\mathcal{Z}}) < \varepsilon$ **then return** $\mathcal{I}_{\mathrm{IR}}$ and **terminate**
3. **while** 1 (processes A) and B))
   - *identify disjointness*: solve the **RDD**:
   - $\Pi^+(\mathcal{E}_{\mathrm{SR}}^{\mathcal{Z}} \backslash \mathcal{I}_{\mathrm{IR}}) = \max_{\boldsymbol{X} \in \mathcal{E}_{\mathrm{SR}}^{\mathcal{Z}}} \min_{\boldsymbol{Y} \in \mathcal{Y}, \boldsymbol{Z} \in \mathcal{Z}, \boldsymbol{S}^+} \{\boldsymbol{1}^{\mathrm{T}}\boldsymbol{S}^+ : \mathrm{s.t.}\ (6), (11)\}$;
   - **if** $\Pi^+(\mathcal{E}_{\mathrm{SR}}^{\mathcal{Z}} \backslash \mathcal{I}_{\mathrm{IR}}) < \epsilon$ **then break**
   - **else** obtain optimal $(\boldsymbol{X}^*, \boldsymbol{Z}^*)$;
   - $i \leftarrow 1$, $\mathcal{I}_{\mathrm{IR},k}^{(1)} \leftarrow \mathcal{E}_{\mathrm{SR}}^{\mathcal{Z}}$, $\mathcal{Z}_{\mathrm{left}}^{(1)} \leftarrow \mathcal{Z}$;
   - **while** 1 (processes a) and b))
     - $\boldsymbol{Z}_{(i)}^* = \arg \min_{\boldsymbol{X} \in \mathcal{I}_{\mathrm{IR}}^{(i)}, \boldsymbol{Y} \in \mathcal{Y}, \boldsymbol{S}^+, \boldsymbol{Z} \in \mathcal{Z}_{\mathrm{left}}^{(i)}} \{\boldsymbol{1}^{\mathrm{T}}\boldsymbol{S}^+ : \mathrm{s.t.}\ (6), (11)\}$;
     - **if** $\boldsymbol{1}^{\mathrm{T}}\boldsymbol{S}^+ > \varepsilon$ **then break**
     - **else** compute $\mathrm{LEC}^{(i)}$ by $(\boldsymbol{X}^*, \boldsymbol{Z}_{(i)}^*)$;
     - $\mathcal{I}_{\mathrm{IR},k}^{(i)} \leftarrow \mathcal{I}_{\mathrm{IR},k}^{(i)} \bigcap \mathrm{LEC}^{(i)}$, $\mathcal{Z}_{\mathrm{left}}^{(i+1)} \leftarrow \mathcal{Z}_{\mathrm{left}}^{(i)} \backslash \boldsymbol{Z}_{(i)}^*$;
     - $i \leftarrow i + 1$;
   - *update logic-based exclusion* constraints by (11);
5. **return** $\mathcal{I}_{\mathrm{IR}}$ and **terminate**

C. Test System Models and Numerical Settings

The numerical experiments are conducted on the modified IEEE 9-bus, 30-bus, and 118-bus test systems. For all cases, the original network topology (bus, branch, and admittance data) is preserved exactly as in the standard IEEE test systems, which

can be obtained from MATPOWER [A1]. Modifications are made only to the unit-commitment-related parameters, includ

ing quick-start capability limits, start-up/shut-down constraints, and generator locations and capacities.

Modification in 9-bus system: The observed SR variables are the branch power flows $P_{\mathrm{B},4-5}$, and $P_{\mathrm{B},8-2}$. The corresponding UC settings for the 9-bus (a) and 9-bus (b) system are listed in Table A-I and Table A-II, respectively, and the active loads are uniformly increased to 1.25 times their original values.

TABLE A-I
MODIFIED UC SETTINGS IN 9-BUS (A) SYSTEM

Generator	Location	$P_{\mathrm{G}}^{\min}$ (MW)	$P_{\mathrm{G}}^{\max}$ (MW)	UC Adjustable (Y/N)
1	Bus 1#	10.000	150.000	Y
2	Bus 1#	50.000	150.000	Y
3	Bus 2#	10.000	300.000	N
4	Bus 3#	10.000	270.000	N

TABLE A-II
MODIFIED UC SETTINGS IN 9-BUS (B) SYSTEM

Generator	Location	$P_{\mathrm{G}}^{\min}$ (MW)	$P_{\mathrm{G}}^{\max}$ (MW)	UC Adjustable (Y/N)
1	Bus 1#	10.000	80.000	Y
2	Bus 1#	100.000	220.000	Y
3	Bus 2#	10.000	300.000	N
4	Bus 3#	10.000	90.000	Y
5	Bus 3#	100.000	180.000	Y

Modification in 30-bus system: The observed SR variables are the branch power flows $P_{\mathrm{B},6-10}$, $P_{\mathrm{B},4-12}$ and $P_{\mathrm{B},28-27}$. The corresponding UC settings are listed in Table A-III, while all other system parameters remain unchanged.

TABLE A-III
MODIFIED UC SETTINGS IN 30-BUS SYSTEM

Generator	Location	$P_{\mathrm{G}}^{\min}$ (MW)	$P_{\mathrm{G}}^{\max}$ (MW)	UC Adjustable (Y/N)
1	Bus 1#	0.000	80.000	N
2	Bus 2#	5.000	80.000	N
3	Bus 13#	5.000	40.000	N
4	Bus 22#	0.000	10.000	Y
5	Bus 22#	15.000	40.000	Y
6	Bus 23#	5.000	30.000	N
7	Bus 27#	0.000	15.000	Y
8	Bus 27#	20.000	40.000	Y

Modification in 118-bus system: The observed SR variables are the branch power flows $P_{\mathrm{B},4-11}$, $P_{\mathrm{B},12-16}$ and $P_{\mathrm{B},23-24}$. The corresponding UC settings are listed in Table A-IV, while all other system parameters remain unchanged.

TABLE A-IV
MODIFIED UC SETTINGS IN 118-BUS SYSTEM

Generator	Location	$P_{\mathrm{G}}^{\min}$ (MW)	$P_{\mathrm{G}}^{\max}$ (MW)	UC Adjustable (Y/N)
1	Bus 10#	0.000	100.000	Y
2	Bus 10#	200.000	550.000	Y
3	Bus 12#	0.000	185.000	N
4	Bus 25#	0.000	320.000	N
5	Bus 26#	0.000	414.000	N
6	Bus 31#	0.000	107.000	N
7	Bus 46#	0.000	119.000	N
8	Bus 49#	0.000	304.000	N
9	Bus 54#	0.000	148.000	N
10	Bus 59#	0.000	255.000	N
11	Bus 61#	0.000	260.000	N
12	Bus 65#	0.000	200.000	Y
13	Bus 65#	50.000	291.000	Y
14	Bus 66#	0.000	200.000	Y
15	Bus 66#	50.000	292.000	Y
16	Bus 69#	0.000	100.000	Y
17	Bus 69#	400.000	805.200	Y
18	Bus 80#	0.000	577.000	N
19	Bus 87#	0.000	104.000	N
20	Bus 89#	0.000	707.000	N
21	Bus 100#	0.000	352.000	N
22	Bus 103#	0.000	140.000	N
24	Bus 111#	0.000	136.000	Y

D. *A single-bus benchmark without any network constraints*

A single-bus benchmark without any network constraints is introduced in this subsection. As illustrated in Fig. A-1, three generators supply a 100 MW load at Bus 1#.

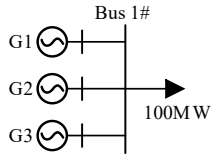

Fig. A-1. Single-bus system.

TABLE A-V
UC SETTINGS I IN SINGLE-BUS SYSTEM

Generator	Location	$P_{\mathrm{G}}^{\min}$ (MW)	$P_{\mathrm{G}}^{\max}$ (MW)	UC Adjustable (Y/N)
G1	Bus 1#	10.000	70.000	N
G2	Bus 1#	10.000	70.000	N
G3	Bus 1#	25.000	60.000	Y

TABLE A-VI
UC SETTINGS II IN SINGLE-BUS SYSTEM

Generator	Location	$P_{\mathrm{G}}^{\min}$ (MW)	$P_{\mathrm{G}}^{\max}$ (MW)	UC Adjustable (Y/N)
G1	Bus 1#	10.000	70.000	N
G2	Bus 1#	10.000	70.000	N
G3	Bus 1#	0.000	100.000	Y

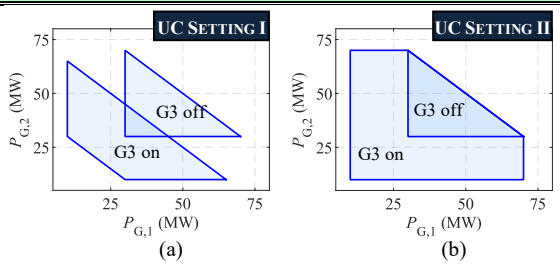

Fig. A-2. (a) SR under UC setting I; (b) SR under UC setting II.

The SR is observed in the space of two decision variables, namely the power injections of G1 and G2, ($P_{\mathrm{G},1}$, $P_{\mathrm{G},2}$). Units G1 and G2 are non-adjustable in the UC stage, whereas G3 is a quick-start UC-adjustable unit whose minimum and maximum limits differ between two UC settings, as specified in TABLE A-VI and TABLE A-VII, respectively.

In UC setting I (TABLE A-VI), the SR with UC adjustments is the union of two SRs corresponding to "G3 on" and "G3 off". Their partial overlap leads to a nonconvex and internally disconnected region in the ($P_{\mathrm{G},1}$, $P_{\mathrm{G},2}$) plane, as shown in Fig. A-2(a). This disjointness arises purely from the discrete on/off status of G3 and the associated change in power balance requirements.

In UC setting II (TABLE A-VII), although the SR is still a union of two SR subsets, the modified capacity limits of G3 make their intersection convex, resulting in a connected SR, as illustrated in Fig. A-2 (b).

The comparison of two UC settings serves as an existence demonstration that UC decisions alone can generate internal disjointness in the SR, even in the complete absence of network constraints. Moreover, in this single-bus system the SR depends on UC-related parameters, in particular the minimum and maximum limits of UC adjustable units, such that some UC parameter settings lead to a connected SR while others create internal infeasible gaps. Consequently, these gaps cannot be attributed solely to network effects.

E. *Sensitivity of the IISI to the accuracy threshold ϵ*

This appendix examines the sensitivity of the proposed IISI method to the accuracy threshold ϵ using the modified IEEE 30-bus system.

TABLE A-VII
TOLERANCE SETTINGS AND CORRESPONDING PERFORMANCE IN THE MODIFIED 30-BUS SYSTEM

Accuracy threshold ϵ	Number of infeasible subregions	Disjointness ratio	Relative error
0.001	32	8.581%	0.000%
0.005	32	8.581%	0.000%
0.010	32	8.581%	0.000%
0.100	28	8.477%	1.212%
1.000	8	5.955%	30.603%

Table A-IV reports the sensitivity of the IISI results to the accuracy threshold ϵ. When $\epsilon \in [0.001,0.010]$, the number of identified infeasible subregions and the disjointness ratio remain unchanged. At $\epsilon = 0.100$, slight underestimation occurs because the refinement process terminates earlier, leading to fewer detected subregions. When $\epsilon = 1.000$, premature termination results in a substantially looser approximation and a noticeable reduction in the identified infeasible volume. These results indicate that a sufficiently small ϵ is needed to accurately capture internal infeasible subregions, whereas larger values mainly reduce the number of iterations at the expense of boundary resolution.

REFERENCES

[A1] R. D. Zimmerman, C. E. Murillo-Sánchez, and R. J. Thomas, "MATPOWER: Steady-state operations, planning, and analysis tools for power systems research and education," *IEEE Trans. Power Syst.*, vol. 26, no. 1, pp. 12-19, Feb. 2011.